Fundamental Spectral Boundaries of Circadian Tunability

J. Cerpentier and Y. Meuret

***Abstract*—The discovery of melanopsin and the non-visual impact of light, lead to a new era in lighting design. Using a melanopic action spectrum, the CIE introduced the melanopic efficacy of luminous radiation (MELR), which quantifies the influence of light on melanopsin. A significant amount of research has been conducted on the possible variation of this MELR and other related metrics for various practical lighting settings, but the fundamental spectral boundaries have not yet been disclosed. Without these limits, it is difficult to assess if a certain lighting system really achieves high or low MELR. This paper determines these fundamental MELR boundaries for different CCT and certain minimal TM-30 R_f values, using a a flexible parametrization of the light source spectrum that is optimized with Differential Evolution. The obtained results show that with increasing CCT, the interval between the theoretical MELR extrema increases slightly, while the opposite occurs when increasing the minimal TM-30 R_f value. The same parametric model and optimization approach is also used to determine the maximal Luminous Efficacy of Radiation (LER) within the obtained MELR limits.**

***Index Terms*—Optimization, non-visual response, spectral power distribution (SPD), melanopic efficacy of luminous radiation (MELR), color, modeling.**

I. Introduction

In this day and age, people spend most of their time indoors, exposed to artificial light [1], [2]. This may disturb the human biological rhythm, and could potentially lead to severe health conditions, such as breast cancer and circadian phase abruption [3], [4]. The circadian rhythm is managed by the suprachiasmatic nucleus (SCN), which can be compared to a clock settled in the human brain [5]. When light falls on the eye, the SCN receives environmental information from the retina through non-image forming, intrinsically photosensitive retinal ganglion cells (ipRGCs), which function as circadian photoreceptors [6], [7]. The ipRGCs express the photopigment melanopsin, which reacts with the incoming light and predominantly influences the excretion of melatonin, a hormone that plays a significant role in sleep cycle moderation [8], [9]. The sensitivity of the ipRGCs to incoming light is known to be wavelength-dependent, and for lighting applications, this is described by a melanopic action spectrum $C(\lambda)$, which peaks at $\lambda_{max} = 490$ nm. $C(\lambda)$ can be considered as the circadian counterpart of the photopic sensitivity function $V(\lambda)$ for human vision [10]. Similar to the widely used $V(\lambda)$, $C(\lambda)$ is standardized by the CIE, and the exact values can be found in CIE S 026/E:2018 [11]. A comparison of $C(\lambda)$ and $V(\lambda)$ is shown in Fig. 1.

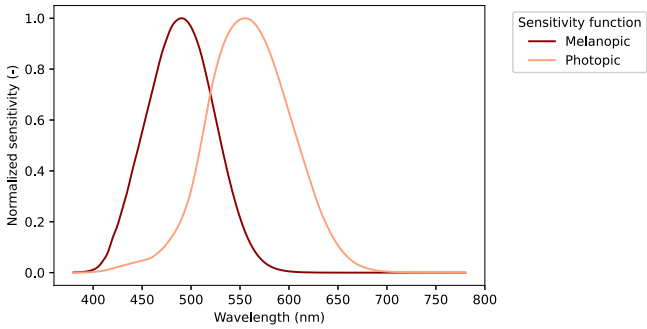

Fig. 1. The melanopic ($C(\lambda)$) and photopic ($V(\lambda)$) sensitivity functions.

The melanopic effect of light plays a significant role in the field of human centric lighting (HCL), which focuses on the design of lighting systems in order to achieve a particular set of visual, biological and behavioral responses to that system [12]. The ipRGCs mainly affect the biological responses, and for a lighting system, its melanopic effect is calculated by studying interactions between the melanopic action spectrum $C(\lambda)$ and the system's spectral power distribution (SPD) $S(\lambda)$. These interactions can be summarized in a metric, and the CIE has standardized the melanopic radiant flux, which is the spectral radiant flux, weighed with the melanopic sensitivity spectrum $C(\lambda)$ [11]. Melanopic radiant flux on its own is useful to quantify circadian effects, but metrics that somehow characterize the ratio of the melanopic to luminous flux are mostly adopted. In particular, CIE S 026/E:2018 defines the melanopic efficacy of luminous radiation (MELR) as:

$$K_{mel,v} = \frac{\int_{380}^{780} S(\lambda)C(\lambda)d\lambda}{K_m \int_{380}^{780} S(\lambda)V(\lambda)d\lambda}, \tag{1}$$

with $S(\lambda)$ the SPD. K_m is the maximum spectral Luminous Efficacy of Radiation (LER) for photopic vision, which is 683.002 $lm \times W^{-1}$, implying that $K_{mel,v}$ is expressed in watts per lumen (W/lm), and thus inherently summarizes the amount of "melanopic" power, relative to the visible light. By considering the shape of $V(\lambda)$ and $C(\lambda)$, it is clear that a higher MELR corresponds to a large amount of energy on the blue side of the source spectrum, while a lower MELR represents a more right-skewed SPD. As in most studies, we will report the MELR in

Manuscript received May 14, 2021; revised July 7, 2021; accepted July 17, 2021. Date of publication July 26, 2021; date of current version August 12, 2021. *(Corresponding author: J. Cerpentier.)*

The authors are with the Department of Electrical Engineering, Light & Lighting Laboratory, KU Leuven, 9000 Ghent, Belgium (e-mail: jeroen.cerpentier@kuleuven.be; youri.meuret@kuleuven.be).

This article has supplementary downloadable material available at https://doi.org/10.1109/JPHOT.2021.3098903, provided by the authors.

Digital Object Identifier 10.1109/JPHOT.2021.3098903

mW/lm, adding another scalar factor of 1000 in the numerator of Equation 1.

Aside from the MELR and melanopic radiant flux, there are various other metrics designed to quantify melanopic effects of light. The circadian action factor (CAF) is calculated as the MELR without the scaling factor K_m in the denominator, and it is widely adopted as the main metric in optimization studies. The CIE also standardized the melanopic daylight efficacy ratio (MDER), which expresses the ratio between the MELR of the source spectrum and the MELR of daylight (D_{65}), which is equal to 1.326 mW/lm. From these definitions, it is clearly seen that the CAF and MDER differ from the MELR only with respect to a scalar factor, in particular:

$$K_{mel,v} = \frac{1000}{683.002} \times \text{CAF} = 1.326 \times \text{MDER}. \tag{2}$$

These relations imply that whenever a study reports CAF or MDER values, it also indirectly provides results on the MELR and vice versa. From the definition of these metrics, it is clear that they solely depend on the shape of the spectrum, and remain identical even after rescaling the SPD, when e.g. performing a normalization to a total power of 1 W. In reality, the melanopic effect of light is not only characterized by the spectral shape, but also by e.g. the total amount of energy falling on the outer surface of the eye. With this in mind, the CIE introduced the melanopic irradiance, which is the spectral irradiance weighted with $C(\lambda)$, and is expressed in watts per square meter ($W \times m^{-2}$). Lastly, this melanopic irradiance can be divided by the earlier mentioned MELR of D_{65} in W/lm, leading to a quantitiy in $lm \times m^{-2}$, which is equivalent to illuminance, expressed in lux (lx), commonly called melanopic lux because of the weighing with $C(\lambda)$. This metric is called the melanopic equivalent daylight illuminance (MEDI). As opposed to the MDER, CAF and MELR, the MEDI does not solely represent biological effects that originate from the spectral shape, but it also accounts for the total amount of light falling on the outer surface of the eye.

Research has shown that even at extremely low melanopic lux levels, melatonin suppression is strongly driven by the ipRGCs and melanopsin. This indicates that appropriate design of SPD's is of high importance, even at low light intensities [9]. With this in mind, this paper solely focuses on melanopic effects that originate from the actual source spectrum. Although the CAF is widely used for this in spectral optimization studies, we adopted the MELR as the main metric of interest, because it is standardized by the CIE; nevertheless, results on the MELR can be easily converted to results on the CAF and MDER, by using 2.

Ideally, the MELR of a light source should correspond with the environmental setting, e.g. energizing light in the morning and relaxing light in the evening. This has lead to a growing interest in dynamic circadian lighting [13]. Such lighting systems realize temporal changes of e.g. the MELR of the emitted light, by combining multiple light sources with different spectra [14], [15]. When varying the circadian impact of the illumination, it is of course important that the other lighting parameters are also controlled to assure high-quality light under all conditions. One essential parameter is the CIE R_a, commonly called the Color Rendering Index (CRI). This metric expresses the ability of a light source to render object colors faithfully when compared to a natural source, but has been argued to be an outdated indicator [16]. An improvement is the IES TM-30 color fidelity (R_f), which uses 99 test color samples for comparison and ranges from 0 to 100 [17], [18]. Another important chromatic lighting parameter is the Correlated Color Temperature (CCT), i.e. the temperature of the planckian radiator whose chromaticity is closest to that of the source [19]. In practice, the CCT is useful because it allows for a quick assessment of a light source's appearance, where lower CCT's correspond to "warm white" light, and higher CCT's to "cool white" light [20]. For the CCT to be a meaningful parameter, the distance to the planckian locus must not be too high. This distance is summarized by the Duv value, which quantifies the distance of the source chromaticity point and the planckian radiator at the calculated CCT in the CIE 1960 chromaticity space. This value thus gives information about the whiteness of the light source [21]. If a source has a high Duv, it may not appear as white anymore.

The importance of these chromatic lighting parameters for artificial light, combined with the interest in dynamic circadian lighting, leads to the question of which MELR values can be obtained by different source spectra with similar chromatic parameters. This knowledge is of practical relevance when designing tunable lighting systems with variable circadian impact that are constrained to certain minimal R_f values or to a specific CCT range. Since the MELR, CAF and MDER only differ scalarly, it suffices to know the MELR minima and maxima in different settings, in order to characterize how these 3 circadian metrics can be tuned under specific chromaticity constraints. These MELR extrema can be found by searching for fitting SPD's. The corresponding SPD's can be acquired through an optimization procedure, by parametrizing the spectrum and optimizing the various parameters with respect to some objective function, also called the merit function. This kind of optimization is called spectral optimization [22], [23]. Using spectral optimization, it has been found that three-band Gaussian SPD's, constrained to a CRI of 80, allow for a decrease or increase of the CAF with respect to the blackbody radiator at a CCT of 2700 K, but only a decrease at 8000K [24]. Another study has shown that obtainable CAF ranges increase when loosening the constraints on R_f and Luminous Efficacy of Radiation (LER), for the specific case of tetrachromatic clusters of narrow-band LEDs [13]. For LED-combinations that aim to maintain white light, with controlled Duv and CCT values and a minimal CRI of 80, it has been found that the CAF is tunable between values of 0.47 and 0.55 [25]. Extrema can also be studied for light sources with varying CCT; for a quantum dot-based six-package LED, the CAF could be tuned from 0.3 to 1.0 while maintaining a minimal R_f of 87.3, by altering the CCT from 2128 K to 6459K [26]. With a parametric model of just 3 parameters, constrained to CRI = 90, it was found that changing the CCT from 2700 K to 6500 K induced a maximal CAF range from 0.294 to 0.957 [27]. In terms of MELR, a recent study showed that under CRI, Duv and TM-30 constraints, a MELR tunablity from 0.43 to 1.82 mW/lm is possible for a 5-channel luminaire, when varying between CCT's of 2700 K and 10000K [28].

While these studies give a first idea of the values that can be achieved with certain practical light sources, and for specific

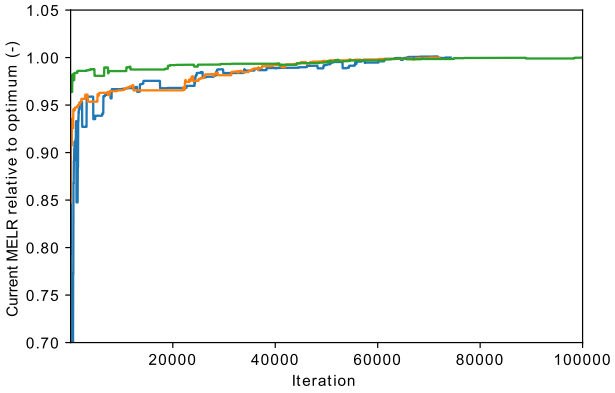

Fig. 2. The obtained MELR value convergences for three different settings. The blue and orange optimization development shows early termination. The green setting does not meet the stopping criterion, but clearly stagnates near the iteration limit.

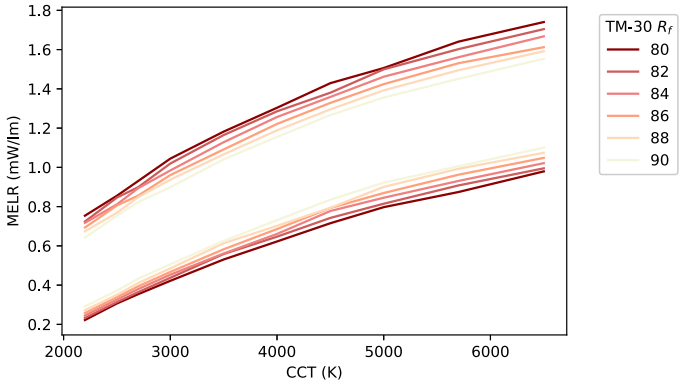

Fig. 3. Maximal and minimal MELR values for the considered R_f contraints, in function of CCT. MELR values increase together with CCT, and the same occurs for the interval width.

chromatic parameters, these do not offer a complete overview of the fundamental spectral limits in terms of CAF, MDER and MELR. Providing these fundamental limits in relation to the chromatic parameters R_f and CCT is the main goal of this paper. To achieve this goal, spectral optimization is performed with SPD's that have the necessary flexibility to attain these fundamental minima and maxima. Furthermore, an advanced optimization algorithm is used, i.e. Differential Evolution (DE), in order to assure that the global extrema are effectively found for all considered settings [29].

II. Methods

We search for fundamental MELR boundaries in different settings. The theoretically maximal (or minimal) MELR in a certain setting will always correspond to a specific SPD that reaches this value. As mentioned in the introduction, these spectra can be found by parametrizing SPD's and optimizing them in terms of the MELR. Since the spectra corresponding to MELR extrema for different chromatic constraints are found to be "unsmooth" and irregular, the parametric model must be flexible enough to be able to reach these spectra. SPD's are generally represented by a sequence of values, corresponding to the spectral radiant flux at each wavelength within the human visible spectrum. In the official CIE documents, $C(\lambda)$ and $V(\lambda)$

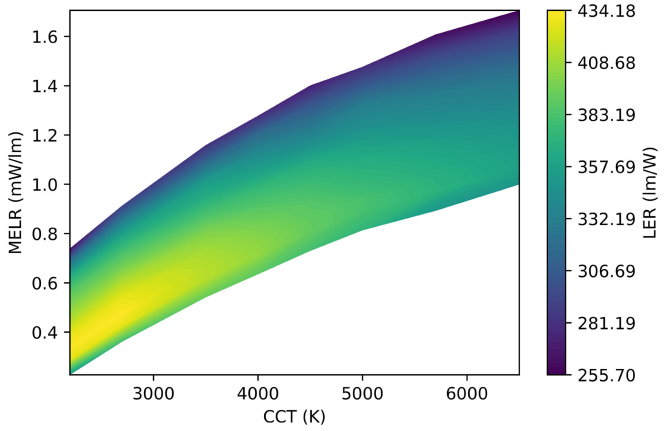

Fig. 4. Maximal LER for each MELR and CCT (with $R_f \geq 80$). A general decrease in maximal LER is visible, as CCT increases. The highest LER values are found below the central MELR.

are also defined in this manner, using wavelength increments of 1 nm, leading to a sequence of 401 values. Since the calculation of the MELR in 1 uses element-wise multiplication of the SPD $S(\lambda)$ with the sensitivity functions $C(\lambda)$ and $V(\lambda)$; describing $S(\lambda)$ as a similar list of 401 values suffices to attain all possible CAF values, including the theoretical boundaries. This implies that spectra should be modelled as a sequence of 401 parameters. This is an extremely high amount, and since we aim to study MELR extrema in various settings (combinations of CCT & R_f), optimizing this model in each setting would take a significant amount of time. To guarantee convergence and consistency, the amount of parameters was reduced to 81, by using steps of 5 nm between consecutive wavelengths. We verified if this induced any loss in achievable MELR values, by optimizing both parametric models with 81 and 401 parameters in 4 different settings, MELR maximization and minimization at 6500 K and 3500 K, under $R_f \geq 90$. The model with a 1 nm interval lead to an average MELR gain of 0.0017%, which is negligible.

The used optimization method in this study, i.e. Differential Evolution, was initially proposed by Storn & Price in 1997 [29]. It is a global optimization algorithm that is considered superior to other algorithms, such as Simulated Annealing [30] or Nelder-Mead optimization [31]. It is a population-based evolutionary algorithm, that modifies a candidate solution with respect to a measure. This makes it a metaheuristic method, capable of optimizing large solution spaces, and therefore it is a good fit for the chosen parametric model and its high amount of parameters [32].

Using the mentioned parametric model, this DE algorithm was used to find the minimal and maximal MELR values for various CCT, various minimal TM-30 R_f and a Duv tolerance which is elaborated further. This was done by minimizing a merit function $f(\mathbf{X})$ with $\mathbf{X}$ the parameter vector of the parametrized SPD model. The constraints on the CCT, R_f and Duv were included in this merit function via penalty terms $p_1(\mathbf{X}), p_2(\mathbf{X})$ and $p_3(\mathbf{X})$. This resulted in the following merit function, depending on whether a MELR minimum or maximum is targeted

$$f(\mathbf{X}) = \pm\text{MELR}(\mathbf{X}) + p_1(\mathbf{X}) + p_2(\mathbf{X}) + p_3(\mathbf{X}). \quad (3)$$

Since the merit function is minimized, a large, positive penalty term is to be added if one of the constraints is not met. For example, the constraint $R_f \geq 80$ was included as the penalty function

$$p_3(\mathbf{X}) = \begin{cases} -1e4 \text{ if } R_f(\mathbf{X}) \geq 80 \\ 1e4 \text{ else} \end{cases}, \quad (4)$$

which was represented in practice as

$$p_3(\mathbf{X}) = 1e4 \times \text{sgn}[\text{sgn}\{80 - R_f(\mathbf{X})\} - 0.5], \quad (5)$$

with sgn() the signum function.

To ensure sufficient whiteness for all considered SPD's, 7-step MacAdam ellipses were considered, which guarantee color consistency according to the ANSI C78.377 standard [33]. This corresponds to a Duv tolerance of 0.006 in both directions. This was included in the optimization constraints by using similar penalties to 4 and 5. Because both MELR and chromatic parameters are independent of the total amount of power, a final optimization constraint restricts the total power to one. This considerably reduces the size of the parameter space.

Minimal R_f value constraints ranged from 80 to 90 with steps of 2 (e.g. $R_f \geq 80$), and the CCT constraints used the values in ANSI C78.377, between 2200 K and 6500 K, where we allowed a deviation of 50 K in both directions. Calculations of CCT, R_f and Duv were performed using the LuxPy package in Python [34]. Because of the high amount of settings in which the MELR is optimized, parallel computing was used to run the optimizations simultaneously [35]. The maximum amount of iterations in the DE algorithm was chosen to be 10^5, and if the algorithm found the same solution for 10^4 consecutive iterations, the procedure was also terminated (tolerance $5e-6$). This high amount of iterations was chosen to address the high dimensionality of the considered optimization problem. Another crucial setting is the DE population size. It has been argued that DE problems with large dimension equal to d, should have a population size anywhere within the interval $[50, 10 \times d]$ [36]. Because this is a large interval, and there is no general consensus on the best population size, two different population sizes were considered in the DE algorithm: the first 5×10^4 iterations work with the largest possibility of $10 \times d$, which equals 810, followed by the remaining 5×10^4 iterations, using a population of size $4 \times d$, which is 324. Fig. 2 illustrates the convergence of three optimizations, relative to the obtained final MELR value. Two out of the three procedures are terminated early by meeting the tolerance criterion of 10^4 iterations. The other procedure also stagnates at the end. These examples illustrate the general convergence of the DE algorithm for this problem, and by being a global optimization algorithm, this also guarantees the non-locality of the obtained solution.

III. Results

The obtained MELR maxima and minima are shown in Fig. 3. It is clear that the interval between maximal and minimal MELR diminishes as the R_f constraint becomes more stringent. This is a logical result, since all spectra that meet $R_f \geq 82$ also meet the less strict condition $R_f \geq 80$. By focusing e.g. on the results for $R_f \geq 80$, it is also visible that the interval size increases as CCT increases. The numerical values for this figure can be found in the supplementary material.

The obtained fundamental MELR boundaries illustrate the well-known fact that MELR can be varied by using SPD's with different CCT. But there is clearly also a significant MELR tunability by using SPD's with similar CCT. The broad MELR intervals for constant CCT are a direct consequence of the spectral flexibility that is offered by the used parametric model, and these are (much) wider than the values that were presented in previous literature for more restricted SPD's, mostly in terms of CAF. The main relevance of these fundamental boundaries lies in the fact that the MELR of any future dynamic circadian lighting system will need to operate within these limits. Knowing these boundaries furthermore allows to evaluate how close a certain dynamic lighting system approaches these fundamental limits.

In terms of CAF, previous research showed that at a CCT of 4000 K with 5 LED channels and a CRI of 80, the CAF could be tuned from 0.47 to 0.55 [25]. With R_f instead of CRI and the same CCT and Duv constraints, we obtained a maximal tunability ranging from 0.43 to 0.89, showing that a significant improvement of the CAF tunability is still possible. In the introduction, it was mentioned that the CAF of a six-package QD-based LED system could be tuned from 0.3 to 1.00 (under $R_f \geq 87.3$) by altering the CCT from ≈ 2200K to ≈ 6500K [26]. By converting the results in Fig. 3 to CAF, it can be seen that for $R_f \geq 88$, the maximal CAF tunability ranges from 0.16 to 1.09 for a CCT alteration of 2200 K to 6500 K. This suggests that the results for the six-package LED approach optimal CAF tunability.

Until this point, we solely focused on maximal MELR tunability. In practice, the Luminous Efficacy of Radiation is also highly relevant. The LER is quantified as the amount of (photopic) lumen divided by the emitted radiant flux in W (lm/W), and it is thus a measure for the amount of visible light with which the considered SPD corresponds [37]. In addition to the resuls in Fig. 3, we thus also studied the maximal achievable LER value in a setting where $R_f \geq 80$, for different CCT's, while varying the MELR in the previously obtained intervals. For each MELR interval at a specific CCT, 10 equally spread values were chosen as target, with an allowed deviation of 2%. The optimization procedure then optimizes LER, with an additional constraint on the MELR. This implies that there are multiple SPD's that can achieve similar MELR, CCT and R_f constraints, and optimization is needed to find the SPD with maximal LER.

Fig. 4 presents the results of the LER optimization. Firstly, by comparing the average maximal LER in the MELR intervals at each CCT, the results indicate that there is a general decrease in maximal obtainable LER with increasing CCT, which had already been suggested in past literature [38]. Second, when fixing the CCT and varying the MELR in the interval, it is clear that the LER values increase when the MELR values decrease. When maximizing the LER, the algorithm forces as much energy as possible around the photopic sensitivity peak, which is easier for lower MELR values. Near the minimal MELR value however, we notice a significant drop in the maximal LER that can be obtained. This is a direct consequence of the low spectral flexibility at the MELR extrema, which is also responsible for the low LER values at the MELR maxima.

Although the LER is widely used as a performance metric for the production of visible light, some consider it to be outdated.

The LER assumes $V(\lambda)$ to be representative for the human eye sensitivity to light, which is only true for higher luminance levels. In future work, it could be relevant to study the relation of MELR boundaries to new criteria that also account for lower luminance levels. Examples are the S/P-ratio, the ratio of scotopic to luminous flux of a light source, or a brightness formula [39]. Another topic of further research is investigating to what extent the identified MELR boundaries in this paper can be reached by current LED- or laser-based light source technologies. In this case, also the electrical-to-optical power efficiency could be taken into account.

IV. Conclusion

In conclusion, this paper presents fundamental spectral limits for the melanopic efficacy of luminous radiation, for various CCT and minimal TM-30 R_f constraints. These fundamental limits were determined by using a flexible parametrization of the SPD's that allows to reach every possible MELR value. This parametric spectrum model was optimized using Differential Evolution. Constraints were imposed on the Duv, CCT and TM-30 R_f. The obtained MELR boundaries can serve as a benchmark for future dynamic circadian lighting systems. The same spectrum parametrization was also used to maximize the attainable LER, within these MELR limits. The results of this optimization show that increasing MELR comes with a strong trade-off in attainable LER, and that reaching minimal or maximal MELR values induces a significant LER penalty.

References

[1] C. J. Matz *et al.*, "Effects of age, season, gender and urban-rural status on time-activity: Canadian human activity pattern survey 2 (chaps 2)," *Int. J. Environ. Res. Public Health*, vol. 11, no. 2, pp. 2108–2124, 2014.

[2] I. Khajehzadeh and B. Vale, "How new zealanders distribute their daily time between home indoors, home outdoors and out of home," *Kōtuitui: New Zealand J. Social Sci. Online*, vol. 12, no. 1, pp. 17–31, 2017.

[3] Y. Cho, S.-H. Ryu, B. R. Lee, K. H. Kim, E. Lee, and J. Choi, "Effects of artificial light at night on human health: A literature review of observational and experimental studies applied to exposure assessment," *Chronobiol. Int.*, vol. 32, no. 9, pp. 1294–1310, 2015.

[4] T. Raap, G. Casasole, R. Pinxten, and M. Eens, "Early life exposure to artificial light at night affects the physiological condition: An experimental study on the ecophysiology of free-living nestling songbirds," *Environ. Pollut.*, vol. 218, pp. 909–914, 2016.

[5] S. M. Reppert and D. R. Weaver, "Coordination of circadian timing in mammals," *Nature*, vol. 418, no. 6901, pp. 935–941, 2002.

[6] S. W. Lockley, G. C. Brainard, and C. A. Czeisler, "High sensitivity of the human circadian melatonin rhythm to resetting by short wavelength light," *J. Clin. Endocrinol. Metab.*, vol. 88, no. 9, pp. 4502–4505, 2003.

[7] C. Dibner, U. Schibler, and U. Albrecht, "The mammalian circadian timing system: Organization and coordination of central and peripheral clocks," *Annu. Rev. Physiol.*, vol. 72, pp. 517–549, 2010.

[8] K. Thapan, J. Arendt, and D. J. Skene, "An action spectrum for melatonin suppression: Evidence for a novel non-rod, non-cone photoreceptor system in humans," *J. Physiol.*, vol. 535, no. 1, pp. 261–267, 2001.

[9] A. S. Prayag, R. P. Najjar, and C. Gronfier, "Melatonin suppression is exquisitely sensitive to light and primarily driven by melanopsin in humans," *J. Pineal Res.*, vol. 66, no. 4, 2019, Art. no. e12562.

[10] J. a. Enezi, V. Revell, T. Brown, J. Wynne, L. Schlangen, and R. Lucas, "A "melanopic" spectral efficiency function predicts the sensitivity of melanopsin photoreceptors to polychromatic lights," *J. Biol. Rhythms*, vol. 26, no. 4, pp. 314–323, 2011.

[11] CIE, "CIE system for metrology of optical radiation for ipRGC-influenced responses to light," 2018, doi: 10.25039/S026.2018.

[12] K. Houser, P. Boyce, J. Zeitzer, and M. Herf, "Human-centric lighting: Myth, magic or metaphor?," *Lighting Res. Technol.*, 2020, Art. no. 1477153520958448.

[13] A. Žukauskas and R. Vaicekauskas, "Tunability of the circadian action of tetrachromatic solid-state light sources," *Appl. Phys. Lett.*, vol. 106, no. 4, 2015, Art. no. 041107.

[14] W. Van Bommel and G. Van den Beld, "Lighting for work: A review of visual and biological effects," *Lighting Res. Technol.*, vol. 36, no. 4, pp. 255–266, 2004.

[15] G. Hoffmann *et al.*, "Effects of variable lighting intensities and colour temperatures on sulphatoxymelatonin and subjective mood in an experimental office workplace," *Appl. Ergonom.*, vol. 39, no. 6, pp. 719–728, 2008.

[16] N. Sandor and H. Yaguchi, "CIE expert symposium on LED light sources: Physical measurement and visual and photobiological assessment," *Color Res. Appl.*, vol. 29, no. 2, p. 168, 2004.

[17] A. David *et al.*, "Development of the IES method for evaluating the color rendition of light sources," *Opt. Exp.*, vol. 23, no. 12, pp. 15888–15906, 2015.

[18] M. P. Royer, "IES TM-30-15 is approved now what?: Moving forward with new color rendition measures," *LEUKOS - J. Illum. Eng. Soc. North Amer.*, vol. 12, no. 1–2, pp. 3–5, 2016. [Online]. Available: http://dx.doi.org/10.1080/15502724.2015.1092752

[19] A. R. Robertson, "Computation of correlated color temperature and distribution temperature," *JOSA*, vol. 58, no. 11, pp. 1528–1535, 1968.

[20] J. Schanda and M. Danyi, "Correlated color-temperature calculations in the CIE 1976 chromaticity diagram," *Color Res. Appl.*, vol. 2, no. 4, pp. 161–163, 1977.

[21] Y. Ohno, "Practical use and calculation of CCT and Duv," *Leukos*, vol. 10, no. 1, pp. 47–55, 2014.

[22] M. Koedam and J. Opstelten, "Measurement and computer-aided optimization of spectral power distributions," *Lighting Res. Technol.*, vol. 3, no. 3, pp. 205–210, 1971.

[23] P. Zhu, H. Zhu, G. C. Adhikari, and S. Thapa, "Spectral optimization of white light from hybrid metal halide perovskites," *OSA Continuum*, vol. 2, no. 6, pp. 1880–1888, 2019.

[24] R. Kozakov, S. Franke, and H. Schöpp, "Approach to an effective biological spectrum of a light source," *Leukos*, vol. 4, no. 4, pp. 255–263, 2008.

[25] T. Aderneuer, O. Stefani, O. Fernández, C. Cajochen, and R. Ferrini, "Circadian tuning with metameric white light: Visual and non-visual aspects," *Lighting Res. Technol.*, to be published, doi: 10.1177/1477153520976934.

[26] H. C. Yoon, J. H. Oh, S. Lee, J. B. Park, and Y. R. Do, "Circadian-tunable perovskite quantum dot-based down-converted multi-package white LED with a color fidelity index over 90," *Sci. Rep.*, vol. 7, no. 1, pp. 1–11, 2017.

[27] Q. Dai, Q. Shan, H. Lam, L. Hao, Y. Lin, and Z. Cui, "Circadian-effect engineering of solid-state lighting spectra for beneficial and tunable lighting," *Opt. Exp.*, vol. 24, no. 18, pp. 20049–20059, 2016.

[28] Y. J. Saw, V. Kalavally, and C. P. Tan, "The spectral optimization of a commercializable multi-channel LED panel with circadian impact," *IEEE Access*, vol. 8, pp. 136498–136511, 2020.

[29] R. Storn and K. Price, "Differential evolution-a simple and efficient heuristic for global optimization over continuous spaces," *J. Glob. Optim.*, vol. 11, no. 4, pp. 341–359, 1997.

[30] S. Kirkpatrick, C. D. Gelatt, and M. P. Vecchi, "Optimization by simulated annealing," *Science*, vol. 220, no. 4598, pp. 671–680, 1983.

[31] J.-m. Renders and S. P. Flasse, "Algorithms for global optimization," *Math. Program.*, vol. 35, no. 1, p. 124, 1986.

[32] S. Das and P. N. Suganthan, "Differential evolution: A survey of the state-of-the-art," *IEEE Trans. Evol. Comput.*, vol. 15, no. 1, pp. 4–31, Feb. 2011.

[33] R. Steen, "Color consistency with LEDs," *Glob. LEDs/OLEDs*, 2011.

[34] K. A. Smet, "Tutorial: The LuxPy Python toolbox for lighting and color science," *Leukos*, 2019.

[35] N. Singh, L.-M. Browne, and R. Butler, "Parallel astronomical data processing with Python: Recipes for multicore machines," *Astron. Comput.*, vol. 2, pp. 1–10, Aug. 2013.

[36] A. P. Piotrowski, "Review of differential evolution population size," *Swarm Evol. Comput.*, vol. 32, pp. 1–24, 2017.

[37] T. W. Murphy Jr, "Maximum spectral luminous efficacy of white light," *J. Appl. Phys.*, vol. 111, no. 10, 2012, Art. no. 104909.

[38] P. Zhong, G. He, and M. Zhang, "Optimal spectra of white light-emitting diodes using quantum dot nanophosphors," *Opt. Exp.*, vol. 20, no. 8, pp. 9122–9134, 2012.

[39] S. A. Fotios and C. Cheal, "Predicting lamp spectrum effects at mesopic levels. Part 1: Spatial brightness," *Lighting Res. Technol.*, vol. 43, no. 2, pp. 143–157, 2011.